

High-resolution 3-D imaging of chronic total occlusions in peripheral vessels using a T-1 weighted Turbo Spin Echo sequence with inner volume imaging

S. Sampath¹, A. N. Raval², R. J. Lederman³, E. R. McVeigh¹

¹Laboratory of Cardiac Energetics, Division of Intramural Research, NHLBI, NIH, DHHS, Bethesda, MD, United States, ²University of Wisconsin, Madison, WI, United States, ³Cardiovascular branch, Division of Intramural Research, NHLBI, NIH, DHHS, Bethesda, MD, United States

Introduction: Peripheral arteries with long totally occluded segments are challenging to maneuver during percutaneous X-ray guided recanalizations due to the absence of a lumen to hold contrast agents (see Fig. 2a) and the tortuous nature of the vessels. High-resolution 3-D volumetric MR imaging that identifies the vascular architecture and the plaque components within may provide pre-procedural information to assist with interventional success. In this abstract, we investigate the use of a T1-weighted 3-D Turbo Spin Echo MRI pulse sequence in combination with inner volume imaging [1,2] to image and characterize occluded arteries within a reasonable clinical acquisition time of around 5-10 minutes with adequate signal-to-noise ratios at 1.5T. Ex-vivo images from animal carotid arteries with an induced chronic total occlusion model and in-vivo images from a patient with atherosclerotic iliac artery occlusion are presented below.

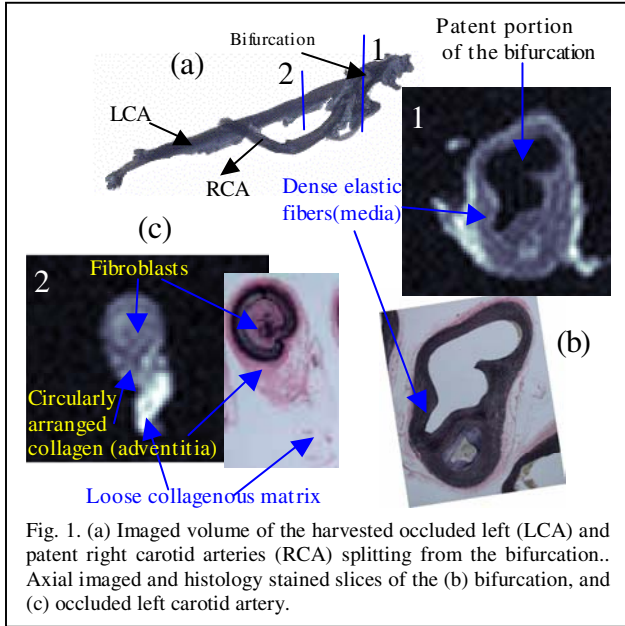


Fig. 1. (a) Imaged volume of the harvested occluded left (LCA) and patent right carotid arteries (RCA) splitting from the bifurcation.. Axial imaged and histology stained slices of the (b) bifurcation, and (c) occluded left carotid artery.

arteries from the pig. Note the common carotid artery bifurcating into the left and the right carotid arteries. Two representative imaged axial slices —1 and 2— and corresponding VVG stained histology sections are also displayed in Fig. 1(c) and (d) (See figure legend for details). It is evident from Fig. 1(b) that a clear distinction between the patent portion and the occluded portion of the bifurcation is achieved. Employing the contrast parameters defined above, we are able to differentiate between loose collagenous matrix (hyper intense), dense elastic fiber (hypo intense), and dense collagenous adventitia(iso intense). The stained section in Fig. 1(c) shows an injured vessel wall with swirling collagen surrounded fibroblasts within the vessel wall. Some features are reproduced in the MR imaged slice depicting plaque structural heterogeneity. The Xray angiogram in Fig. 2(a) depicts the length of the occlusion in the patient's left iliac artery just after the bifurcation. A small volume of interest indicated by the red box in (a) was imaged. The imaged sagittal slice Fig. 2(b) demonstrates good flow suppression in the vessel discriminating between patent and occluded segments. A series of axial sections of this imaged volume in Fig. 2(d) also shows the presence of an obstructed lumen and the compositional variability in the imaged plaque is captured by the heterogeneity in signal intensity in our images. The boundaries of the vessel wall and the lesions were traced out on axial images, which were then smoothed and reconstructed (See Fig. 2(c)) to help identify the position of this obstruction within the selected volume of interest.

Conclusion: A T1-W 3D TSE sequence with inner volume imaging provides a clinically fast method to obtain high-resolution imaging of the heterogeneity of plaque components in tortuous CTO vessels with a view toward practical percutaneous revascularization.

References:

1. Feinberg D.A. et al, Radiology. 1985 156:743-747.
2. Crowe et al, JMRI. 2005 Oct;22(4):583-8.

Imaging Technique: All experiments were performed on a 1.5 T Siemens Sonata scanner. The pulse sequence images a tubular rectangular volume with the long axis in the readout direction along the vessel. For each TR, a slice-selective 90°-excitation pulse was first used to saturate the spins within a user-defined slab thickness along the partition-encode direction. This was then followed by a series of 180°-refocusing pulses designed to be slice-selective along the phase-encode direction thus refocusing only those spins that lay within the volume of intersection of the two orthogonally selected slabs. This technique substantially decreases the phase-encode FOV requirements. The FOV in the phase and partition encode directions were selected to be ~30% larger than the slab thickness to compensate for imperfect rectangular slab profiles. The k-space was sampled in a Cartesian segmented interleaved fashion, with the center of k-space being sampled at the user-selected TE. The zeroth moment of the read-out gradients were nulled at the center of each refocusing echo to achieve flow compensation along the readout direction. The phase encode and partition encode gradients were rewound before the next refocusing pulse was played out to ensure equal phase on all stimulated echo signals generated by the echo train. Crusher gradients were played out at the end of the acquisition window every TR. The sequence was tested on an ex-vivo sample of carotid arteries harvested from a high lipid fed pig with a predominantly patent right carotid artery and with a chronic total occlusion (CTO) model induced by balloon injury in the left carotid artery. The sample was later sent for histology staining (Verhoff Van Gieson (VVG) & Masson Trichrome) to classify lesion composition on axial slices. A patient with a CTO in the left iliac artery was also scanned to assess feasibility of this approach to differentiate between the patent and occluded portions of the vessel and to further identify heterogeneous plaque components. For the pig/patient data presented below, the key imaging parameters used were: TurboFactor:7/7, TR:300/500ms, TE:9/17ms, ReadFOV:192/250mm, PhaseFOV:66/62.5mm, Slab thickness: 30/28.8mm, Isotropic volumetric resolution: 0.5mm³/0.8mm³.

Results and Discussion: Fig. 1 (a) shows the imaged volume of the harvested carotid arteries from the pig. Note the common carotid artery bifurcating into the left and the right carotid arteries. Two representative imaged axial slices —1 and 2— and

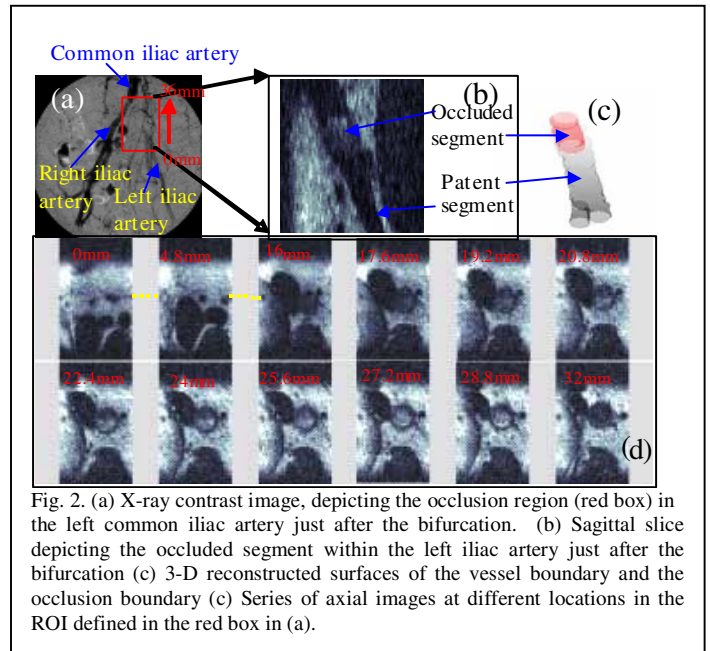


Fig. 2. (a) X-ray contrast image, depicting the occlusion region (red box) in the left common iliac artery just after the bifurcation. (b) Sagittal slice depicting the occluded segment within the left iliac artery just after the bifurcation (c) 3-D reconstructed surfaces of the vessel boundary and the occlusion boundary (c) Series of axial images at different locations in the ROI defined in the red box in (a).